Sborník vědeckých prací Vysoké školy báňské - Technické univerzity Ostrava
číslo 1, rok 2009, ročník IX, řada stavební
článek č.2

Miroslav ROSMANIT[1], Monique C.M. BAKKER[2]

POST-BUCKLING STRENGTH OF UNIFORMLY COMPRESSED PLATES

POKRITICKÁ ÚNOSNOST ROVNOMĚRNĚ TLAČENÝCH STĚN

Abstract

This paper focuses on the development of simple models for describing the influence of initial out-of-plane imperfections on the post-buckling strength of square uniformly compressed plates without stiffeners. This is the first step in gaining a better understanding of the behavior of compression flanges of cold-formed steel members, necessary for the development of new, accurate and insight providing design rules for first and second generation trapezoidal profiled sheeting, subjected to the combined action of a concentrated load (support reaction) and a bending moment.

Abstrakt

Předmětem článku je vývoj jednoduchého modelu popisujícího pokritické chování čtvercových rovnoměrně tlačených nevyztužených stěn se zahrnutím vlivu počátečních imperfekcí. Tento výzkum může být chápán jako první krok pro lepší pochopení chování tlačených stěn tenkostěnných ocelových profilů, je nezbytný pro vývoj nového přesného a zároveň jednoduchého výpočetního postupu pro návrh první a druhé generace trapézových plechů namáhaných kombinací zatížení osamělým břemenem a ohybovým momentem (v místě nad vnitřní podporou).

1 INTRODUCTION

In this paper the post-buckling failure behavior of square plates is studied. All edges of the plate are simply supported ($u_z = 0$). The edges loaded by the compression force are forced to remain straight, but free to experience Poisson's contraction. The other two edges are free to wave in-plane, thus membrane stresses in the y-direction are equal to zero. These boundary conditions correspond to the boundary conditions usually used for the modeling of compression flanges in thin-walled steel deck sections. The research is focused on the strength of cold-formed deck sections subjected to the combined action of bending moment and concentrated load (Hofmeyer *et al*; 2001 and 2006). The concentrated load causes deformations of the compression flange which are large. Therefore it was decided to study the failure behavior of uniformly compressed plates with initial imperfections.

When a perfectly flat simply supported plate is subjected to uniaxial compression, the stress distribution is uniform over the plate, until the buckling load is reached. After buckling the stress distribution becomes non-uniform, both over the width b and the length a of the plate. Plate with unloaded edges forced to remain straight but free to move in-plane have the same buckling load, but differ in their post-buckling behavior. For plates with initial imperfections the stress distribution is non-uniform from the onset of loading. In this paper, it is assumed that the plate has a sinusoidal initial imperfection, with the maximum imperfection occurring at the center of the plate, see Fig. 1.

[1] Ing. Miroslav Rosmanit, Ph.D., Katedra konstrukcí, Fakulta stavební, VŠB-Technická univerzita Ostrava, VŠB - Technická univerzita Ostrava, Fakulta stavební (FAST), Ludvíka Podéště 1875/17, 708 33 Ostrava - Poruba, tel.: (+420) 597 321 398, e-mail: miroslav.rosmanit@vsb.cz.

[2] dr. ir. M.C.M. Bakker, Department of Architecture, Building and Planning, Technische Mechanica, TU/e Technische Universiteit Eindhoven, P.O. Box 513, 5600 MB EINDHOVEN, tel.: (+31) 40 2472203, e-mail: m.c.m.bakker@bwk.tue.nl.

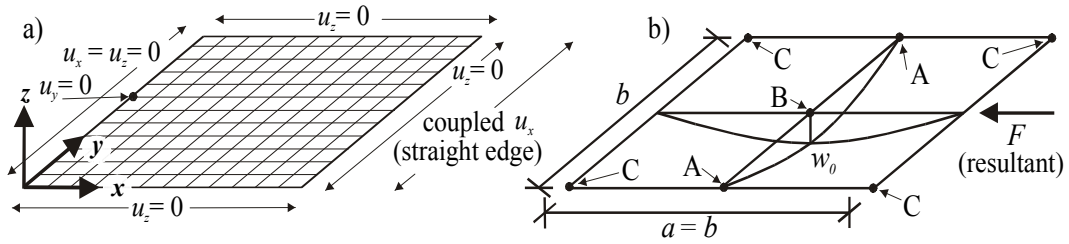

Fig. 1: Schematic view of numerical model:
a) Boundary conditions;
b) Initial imperfection, load, measures and location of points A and B and C. Point A is located in the middle fibers, points B and C are located in outer fibers which are most compressed.

In this paper the following results will be discussed:

- the load F or average stress in x-direction: $\sigma_{x;av} = F/(bt)$;
- the axial shortening u or the average strain in x-direction: $\varepsilon_{x;av} = u/a$;
- membrane stresses $\sigma_{x;A}$ in the x-direction at point A.

These results will be presented as functions of the out-of-plane deflection w at the center of the plate, where w is the total out-of-plane deflection at the center of the plate, including the initial imperfection w_0. These results can be made dimensionless by using the buckling stress:

$$\sigma_{cr} = \frac{K\pi^2 D}{b^2 t} \tag{1}$$

from which we can define the critical strain: $\varepsilon_{cr} = \frac{\sigma_{cr}}{E}$ (2)

the critical axial shortening: $u_{cr} = \varepsilon_{cr} a = \frac{\sigma_{cr} a}{E}$ (3)

and the critical load: $F_{cr} = bt\sigma_{cr}$ (4)

and D is the plate flexural rigidity factor: $D = \frac{Et^3}{12\left(1-\nu^2\right)}$ (5)

t is the plate thickness, a and b are the length and width of the plate (for a square plate $a = b$), E is the modulus of elasticity and K is the buckling coefficient (for a square plate $K = 4$), and v is Poisson's ratio.

According to Little (1980), for two plates having the same values of v, a/b, b/t, $\sqrt{(f_y/E)}$ (or f_y/σ_{cr}) and w_0/t, but different values of f_y, E, and w_0/b, numerical analysis will predict precisely the same non-dimensional load-shortening response. Tab. 1 gives an overview of the material and plate properties which were kept constant in the parameter study. The critical stress was varied in five steps between f_y and $f_y/8$ by varying the width b of the plate. For each plate 7 different imperfections were considered ($0.01t$, $0.1t$, $0.25t$, $0.5t$, t, $1.5t$, and $2t$). Each simulation with the finite element program ANSYS 8.1 has been performed once with linear-elastic material properties, and once with linear-elastic/ideal plastic (bilinear) material properties. All boundary conditions, axis convention and the specific points on the plate are presented in Fig. 1. In the model rectangular elements Shell43 were used. The mesh density for each plate was 40 x 40 elements. In the calculations the effect of large deformations was included.

Tab. 1: Input data for performed numerical (FEM) parameter study.

constant properties			critical stresses	determined values, see eqs. (1) – (4)			
			σ_{cr} [N/mm^2]	b [mm]	b/t [-]	F_{cr} [N]	u_{cr} [mm]
f_y	[N/mm^2]	300	f_y	35.2	50.3	7392.0	$5.021.10^{-2}$
t	[mm]	0.7	$2f_y/3$	40.7	58.1	6410.3	$4.361.10^{-2}$
ν	[-]	0.3	$f_y/2$	49.8	71.1	5229.0	$3.557.10^{-2}$
E	[N/mm^2]	$2.1.10^5$	$f_y/4$	70.4	100.6	3696.0	$2.514.10^{-2}$
D	[Nmm]	6596	$f_y/8$	99.6	142.3	2614.5	$1.779.10^{-2}$

2 RESULTS OF FINITE ELEMENT SIMULATIONS

Fig. 2 gives an overview of the elastic and elasto-plastic behavior of the investigated plates obtained from the performed finite element simulations. In this Fig. 2 the solid dots indicate the ultimate loads. The meaning of the other symbols is discussed later in this paper.

The finite element simulations showed that for most cases first yield occurs in the outer fibers in an area near the corners of the plate (point C). Yielding continues along the longitudinal plate edge, with first membrane yield occurring at the midpoint of the longitudinal edges (point A). Failure is not at first membrane yield but after some membrane yielding of the plate edges. At failure the outer fibers in the center of the plate (point B) do not yield yet. This type of failure is ductile in nature and results in a failure load which may be significantly larger than the load corresponding to first membrane yield at the plate edge. It was also found that outer fiber yield at the corner hardly influences the load-deformation behavior. The elasto-plastic load-deformation behavior starts to deviate from the elastic behavior only after first membrane yield. This type of failure will be denoted further as failure by membrane yielding.

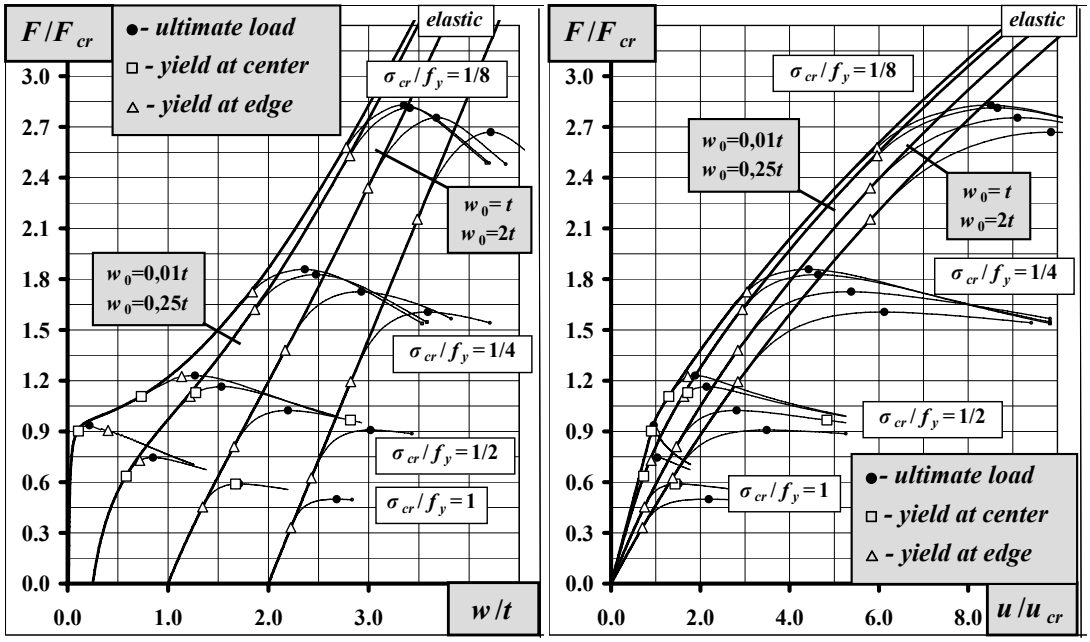

Fig. 2: Overview of selected curves obtained from the FEM simulations.

For the specific case of a plate with both small imperfections and a buckling stress close to the yield stress, first yield occurs in the outer fibers of the center of the plate (point B), resulting in an immediate deviation of the elasto-plastic load-deformation behavior from the elastic behavior. Next the outer fibers in an area near the corners of the plate (point C) start yielding. The ultimate load may

be reached before or after first membrane yield at point A. This type of failure is more violent, and may result in a load which may be either smaller or larger than the elastic load corresponding to first membrane yield. This type of failure will be denoted further as failure by outer fiber yield.

3 PREDICTION OF FAILURE LOADS

According to Rhodes (1982) the maximum load a plate can withstand is very close to the elastic load causing first membrane yield at point A. This assumption is also the starting point for strength predictions based on the effective width approach. According to Calladine (1985), failure occurs when the outer fibers in the center of the plate (at point B) start yielding. In this paper it is proposed to develop different models to predict failure by membrane yielding respectively failure by outer fiber yield. According to Rhodes (1982) the maximum load a plate can withstand is very close to the elastic load causing first membrane yield at point A. This assumption is also the starting point for strength predictions based on the effective width approach. According to Calladine (1985), failure occurs when the outer fibers in the center of the plate (at point B) start yielding. In this paper it is proposed to develop different models to predict failure by membrane yielding respectively failure by outer fiber yield.

Failure by membrane yielding is defined to occur in plates where first membrane yield at the midpoint of the longitudinal edges (point A) occurs before outer fiber yield at the center of the plate. To model the additional elasto-plastic strength after first membrane yield (which is disregarded in the effective width approach), the assumption is made that the plates fail at an average applied strain equal to the yield strain (or at in-plane shortening equal to f_y/σ_{cr} times the critical shortening).

Failure by outer fiber yield at the plate center is defined to occur in plates where outer fiber yield at the plate center occurs before first membrane yield. For this type of failure it was surprisingly found that the elastic load corresponding to first membrane yield at the edge results in a good prediction of the failure load, better than the elastic load corresponding to first outer fiber yield in the center of the plate. It is possible that taking the first-yield condition not at the surface of the plate but at a point positioned somewhat inwards to the middle surface (as proposed by Calladine 1985), will result in even better prediction of the ultimate load.

According to Mahendran (1997), outer fiber yield at the center of the plate will occur before first membrane yield if:

$$w_0 / t \le 0.67 + 0.086S - 0.081S^2 \tag{6}$$

with

$$S = (b/t)\sqrt{f_y / E} \tag{7}$$

This formula agreed with the performed finite element simulations and can thus be used to determine whether the plate will fail by outer fiber yield or by membrane yield. Note that in the derivation of this equation, as well as in the modified strip model it is assumed that outer fiber yield in an area near the corners of the plate (point C) does not affect the load-deformation behavior of the plates.

In the next sections it will be described how the elastic load corresponding to first membrane yield (indicated as open triangles in Fig. 2) and the elasto-plastic load corresponding to an average in-plane strain equal to the yield strain can be determined with a modification of a strip model originally proposed by Calladine (1985).

4 ELASTIC BEHAVIOR ACCORDING TO THE MODIFIED STRIP MODEL

The elastic post-buckling behavior of thin plates with initial imperfections is governed by Marguerre's equations. Bakker et al (2006) and Rosmanit and Bakker (2006-a), showed that the elastic load-deformation behavior of uniformly compressed square plates under load up to three times the critical load can accurately be described by a modification of a large deflection solution given by Williams and Walker (1975):

$$\frac{F}{F_{cr}} = \frac{\sigma_{x;av}}{\sigma_{cr}} = (1 - \frac{w_0}{w}) + A_F\,\eta + B_F\,\eta^2 \tag{8}$$

$$\frac{u}{u_{cr}} = \frac{\varepsilon_{x;av}}{\varepsilon_{cr}} = \left(1 - \frac{w_0}{w}\right) + A_u\eta + B_u\eta^2 \tag{9}$$

with
$$\eta = \left(\frac{w}{t}\right)^2 - \left(\frac{w_0}{t}\right)^2 \tag{10}$$

where
$$A_F = 0.2356,\ B_F = -0.3140.10^{-2},\ A_u = 0.5775,\ B_u = 0.7800.10^{-2} \tag{11}$$

For the small deflection range (loads up to 1.5 times the buckling load) the coefficients B may be taken zero. The resulting equations then correspond to the equations given by Rhodes (1982).

Calladine (1985) used a simple two-element model to represent the behavior of a plate (see Fig. 3). In this model there are two edge strips with a total width bed that always remain straight, and one central strip with a width $b_{ce} = b - b_{ed}$ which behaves like a classical Euler column (i.e. it buckles at constant stress, equal to the buckling stress σ_{cr} of the full plate). According to this model the total load carried by the plate can be calculated as:

$$F = b_{ed}\sigma_{ed}t + (b - b_{ed})\sigma_{ce}t \tag{12}$$

$$\frac{F}{F_{cr}} = \frac{\sigma_{x;av}}{\sigma_{cr}} = \frac{b_{ed}}{b}\frac{\sigma_{ed}}{\sigma_{cr}} + \frac{b - b_{ed}}{b}\frac{\sigma_{ce}}{\sigma_{cr}} \tag{13}$$

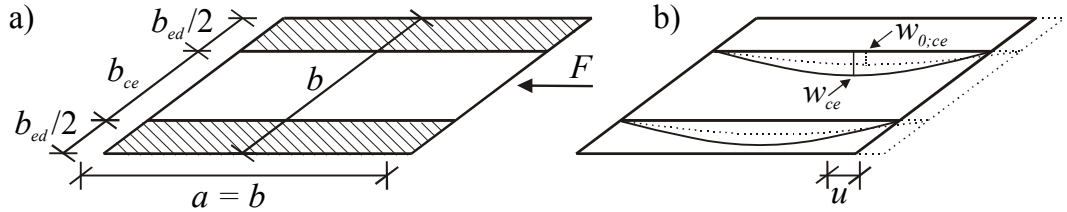

Fig.3: a) Strip and b) deformed strip model of the compressed plate by Calladine (1985).

The strain of the central strip can be calculated as the sum of the elastic compressive strain and the geometric strain ε_g:

$$\frac{\varepsilon_{ce}}{\varepsilon_{cr}} = \frac{\sigma_{ce}}{E\varepsilon_{cr}} + \frac{\varepsilon_g}{\varepsilon_{cr}} = \frac{\sigma_{ce}}{\sigma_{cr}} + \frac{\varepsilon_g}{\varepsilon_{cr}} \tag{14}$$

where ε_g is calculated from the shortening u of the central strip due to out-of-plane deflections (in the shape of a half-sine wave):

$$\varepsilon_g = \frac{u}{a} = \frac{\pi^2(w_{ce}{}^2 - w_{0;ce}^2)}{4a^2} \tag{15}$$

The central strip behaves like an Euler column, so that the imperfection amplification factor $\xi = w_{ce}/w_{0;ce}$ can be determined as:

$$\xi = \frac{n}{n+1} \tag{16}$$

$$n = \frac{\sigma_{ce}}{\sigma_{cr}} \tag{17}$$

Eq. (16) can be used to calculate the membrane stress in the central strip as a function of the out-of-plane deflection of the plate:

$$\frac{\sigma_{ce}}{\sigma_{cr}} = (1 - 1/\xi) = 1 - \frac{w_{0;ce}}{w_{ce}} \tag{18}$$

Calladine (1985) assumed that the maximum lateral deflections w and w_0 of the plate are equal to the maximum lateral deflections w_{ce} and $w_{0;ce}$ of the central strip. In this paper it will be assumed that the maximum deflection (respectively maximum initial deformation) of the central strip can be related to the plate deformations by a scalar $\sqrt{C_w}$ as:

$$w_{ce} = \sqrt{C_w}\, w \tag{19}$$

$$w_{0;ce} = \sqrt{C_w}\, w_0 \tag{20}$$

Using eqs. (15), (18), (19) and (20), eq. (14) can be rewritten to give:

$$\frac{\varepsilon_{ce}}{\varepsilon_{cr}} = (1 - \frac{w_0}{w}) + \frac{C_w 3(1-\nu^2)b^2}{a^2 K}\eta \tag{21}$$

Calladine's model was developed for the small-deflection range. It can be shown that for elastic edge strip and elastic central strip behavior the modified strip model and the small-deflection model (eqs. (8) and (9), with $B_F = B_u = 0$) give identical strains if:

$$C_w = \frac{A_u a^2}{3(1-\nu^2)b^2} \tag{22}$$

Compatibility requires that the strain in the edge strip equals the strain in the central strip:

$$\varepsilon_{ed} = \varepsilon_{ce} = \varepsilon_{x;av} \tag{23}$$

The stress in the edge strip can be calculated as:

$$\sigma_{ed} = E\varepsilon_{ed} \tag{24}$$

Using eqs. (18) to (24), eq. (13) can be written as:

$$\frac{F}{F_{cr}} = \left(1 - \frac{w_0}{w}\right) + \frac{b_{ed}}{b} A_u \eta \tag{25}$$

Comparing Eq. (25) with eq. (8) in the small deflection range (taking $B_F = 0$), it can be seen that these two equations give identical results if:

$$\frac{b_{ed}}{b} = \frac{A_F}{A_u} \tag{26}$$

The modified strip model can also be used in the large-deflection range by using eq. (9) instead of (21) to describe the strain, resulting in:

$$\frac{F}{F_{cr}} = \left(1 - \frac{w_0}{w}\right) + \frac{b_{ed}}{b}\left(A_u \eta + B_u \eta^2\right) \tag{27}$$

Eqs. (27) and (8) give identical results if:

$$\frac{b_{ed}}{b} = \frac{A_F \eta + B_F \eta^2}{A_u \eta + B_u \eta^2} \tag{28}$$

Thus it can be concluded that the modified strip method gives identical results to eqs. (8) and (9).

5 PREDICTION OF ELASTIC LOAD CORRESPONDING TO FIRST MEMBRANE YIELD

In section 4 the membrane stresses are assumed to be constant over the width of the strips. A more accurate membrane edge stress can be calculated by taking σ_{ed} and σ_{ce} equal to the average stress over edge and central strip and assuming a linear stress distribution over the edge strip and a parabolic stress distribution in the central strip. Note that this model is different from Calladine's (1985) model which assumed that the stress in the edge strip equals the membrane stress at the edges of the plate ($\sigma_{ed} = \sigma_{x;A}$), see Fig. 4.

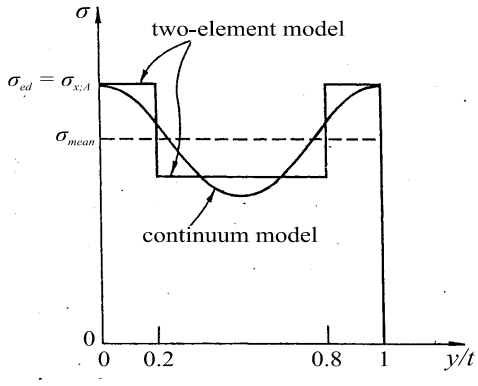

Fig. 4: Model of stress distribution over the central cross section (Calladine, 1985). The stresses at the edges of the plate, and the mean stress in the plate, are the same for both continuum and two-element models.

By requiring that the stresses and the stress gradients are continuous at the border between central strip and edge strip (see Fig. 5), the membrane stress at the edge of the plate can be calculated as:

$$\sigma_{x;A} = \sigma_{ed} + \Delta\sigma_{ed} \tag{29}$$

with

$$\Delta\sigma_{ed} = \left(\sigma_{ed} - \sigma_{ce}\right) \Big/ \left(1 + \frac{2}{3}\frac{b_{ce}}{b_{ed}}\right) \tag{30}$$

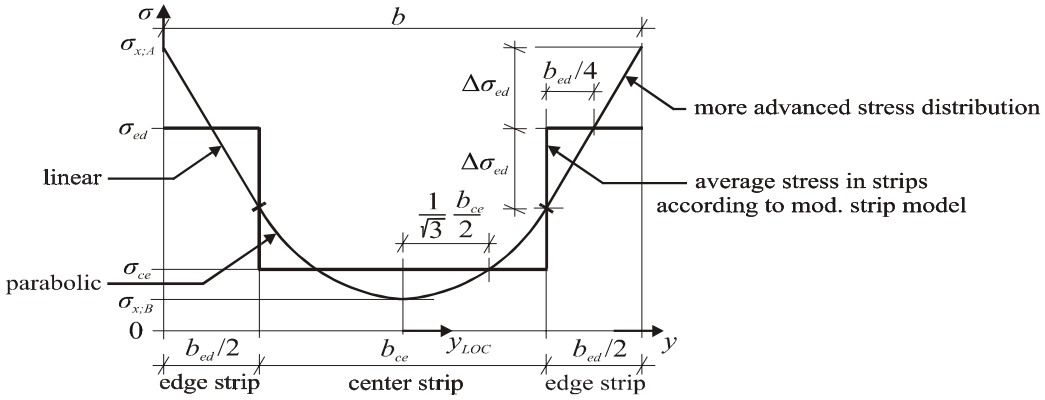

Fig. 5: Two models of stress distribution over the central cross section.

By using a series expansion of $\sigma_{x;A}/\sigma_{cr}$ around the point $\eta = 0$ and leaving out negligible small terms eq. (29) can be further simplified to get:

$$\frac{\sigma_{x;A}}{\sigma_{cr}} = \left(1 - \frac{w_0}{w}\right) + A_{\sigma x;A}\eta + B_{\sigma x;A}\eta^2 \tag{31}$$

where

$$A_{\sigma x;A} = 0.8710 \text{ and } B_{\sigma x;A} = -0.5223.10^{-2} \tag{32}$$

From eq. (31) the deflection $w_{fy;A}$ corresponding to first membrane yield ($\sigma_{x;A} = f_y$) can be solved (by trial and error). Then the load corresponding to this deflection can be calculated from eq. (8). The thus determined elastic loads $F(w_{fy;A})$ are indicated with open triangles in Fig. 2, and can be used to predict failure by outer fiber yield as explained in section 3.

6 PREDICTION OF ELASTO-PLASTIC LOAD CORRESPONDING TO FIRST YIELD STRAIN

To determine the elasto-plastic load corresponding to an average in-plane strain equal to the yield strain the following model is proposed. First the deflection $w_{\varepsilon y}$, corresponding to $\varepsilon_{x;av} = \varepsilon_y = f_y / E$ is solved (by trial and error) from eq. (9). Using this deflection the elastic load $F(w_{\varepsilon y})$ and the stress difference $\Delta\sigma_{ed}(w_{\varepsilon y})$ are calculated from equations (8) respectively (30). Then the stress resultant $\Delta F(w_{\varepsilon y})$ of all stresses larger than the yield stress is calculated (33). Using this stress resultant the elasto-plastic load corresponding to the yield strain can be determined (34). The thus determined loads can be used to predict failure by membrane yield as explained in section 3. Elastic strain behavior remains valid in a plastic range, see Rosmanit and Bakker 2006-a.

$$\Delta F(w_{\varepsilon y}) = \tfrac{1}{4} b_{ed} t \, \Delta\sigma_{ed}(w_{\varepsilon y}) \tag{33}$$

$$F_{ep}(w_{\varepsilon y}) = F(w_{\varepsilon y}) - \Delta F(w_{\varepsilon y}) \tag{34}$$

7 COMPARISON OF RESULTS AND CONCLUSIONS

The final results are presented in Tab. 2. The first column shows an overview of the results from numerical calculations by presenting the ratios of the ultimate loads to the critical loads for the full set of performed calculations. The second and third column show the ratios of the elastic loads corresponding to first membrane yield (according to (31) and (8)) respectively the elasto-plastic loads corresponding to the yield strain (according to (34)) to the ultimate loads calculated by ANSYS. The arithmetic means and coefficients of variations are also calculated, one for the shaded and one for the non-shaded cells.

Tab. 2: Errors in calculations of ultimate load.

	$F_{u;ANSYS}/F_{cr}$					$F(w_{fmv})/F_{u;ANSYS}$					$F_{ep}(w_{\varepsilon y})/F_{u;ANSYS}$				
	σ_{cr}					σ_{cr}					σ_{cr}				
w_0	f_y	$2f_y/3$	$f_y/2$	$f_y/4$	$f_y/8$	f_y	$2f_y/3$	$f_y/2$	$f_y/4$	$f_y/8$	f_y	$2f_y/3$	$f_y/2$	$f_y/4$	$f_y/8$
0.01*t*	0.94	1.02	1.23	1.86	2.83	1.03	1.06	1.02	0.94	0.93	1.04	1.09	1.09	1.05	1.04
0.10*t*	0.82	0.96	1.20	1.85	2.83	1.04	1.03	1.00	0.93	0.92	1.08	1.09	1.07	1.04	1.03
0.25*t*	0.75	0.90	1.16*	1.83	2.81	0.99	0.98	0.95*	0.91	0.91	1.06	1.06	1.05*	1.02	1.02
0.50*t*	0.68*	0.83	1.11	1.79	2.79	0.90*	0.90	0.89	0.87	0.89	1.02*	1.02	1.02	1.00	1.01
1.00*t*	0.59	0.74	1.02	1.73	2.75	0.78	0.79	0.80	0.82	0.86	0.94	0.95	0.96	0.97	0.98
1.50*t*	0.54	0.69	0.96	1.66	2.71	0.72	0.73	0.75	0.78	0.83	0.90	0.91	0.93	0.94	0.96
2.00*t*	0.50	0.64	0.91	1.61	2.67	0.69	0.70	0.73	0.76	0.81	0.88	0.89	0.91	0.93	0.95
arithmetic mean						0.99	1.02	0.99	-	-	1.05	1.08	1.07	-	-
coefficient of variation						0.07	0.04	0.04	-	-	0.03	0.01	0.02	-	-
arithmetic mean						0.73	0.78	0.79	0.86	0.88	0.91	0.94	0.95	0.99	1.00
coefficient of variation						0.06	0.11	0.09	0.08	0.05	0.04	0.06	0.05	0.05	0.03

- The shaded cells represent failure by outer fiber yield – according to Mahendran (1997).

- The non-shaded cells represent failure by membrane yield – according to Mahendran (1997).

* Marked cells represent failure by membrane yield – according to ANSYS.

For plates failing by membrane yielding the elasto-plastic load corresponding to the yield strain results in a more accurate, less conservative prediction of the ultimate load than the elastic load corresponding to first membrane yield (as used in the effective width method). It can be seen that the proposed method slightly overestimates the elasto-plastic loads for small initial imperfections and slightly underestimates them for large initial imperfections.

For plates failing by outer fiber yield the elastic load corresponding to first membrane yield results in a good prediction of the failure load with respect to the average value.

To distinguish between failure by membrane yielding and failure by outer fiber yield formulas (6) and (7) derived by Mahendran (1997) can be used. As the marked (*) cells in Tab. 2 show, the Mahendran formulas for some cases predicts failure by outer fiber yield, where the ANSYS results indicate failure by membrane yield. Improvement of the Mahendran formulas may be possible, but therefore a more rigorous parameter study is needed.

Note that some more results on this project can be found in Rosmanit and Bakker (2006-b).

NOTATION

A_i, B_i	coefficients
D	plate flexural rigidity factor, see (5)
E	Young's modulus of elasticity
F	load – compression longitudinal force
F_{cr}	critical load, see (4)
K	buckling coefficient
a, b	plate length/width; for a square plate $a = b$
b_{ce}, b_{ed}	width of the centre respectively edge strip, see Figs. 3 and 5
t	plate thickness
u, u_{cr}	axial shortening respectively critical axial shortening
w, w_0	total respectively initial out-of-plane deflection at the centre of the plate
ε_{ce}, ε_{ed}	average strain at centre respectively edge strip according to σ_{ce}, σ_{ed}
ε_{cr}	critical strain of the plate, see (2)
ε_g	geometric strain, see (15)
$\varepsilon_{x;av}$	average strain in x-direction, $\varepsilon_{x;av} = u/a$
η	dimensionless parameter, depends on w, w_0 and t, see (10)
υ	Poisson's ratio
ξ	imperfection amplification factor, see (16)
σ_{ce}, σ_{ed}	average membrane stress at centre respectively edge strip, see Fig. 5
σ_{cr}	critical stress of the plate, see (1)
$\sigma_{i;j}$	membrane stress on direction i at point j
$\sigma_{x;av}$	average stress in x-direction, $\sigma_{x;av} = F/(bt)$

ACKNOWLEDGMENT

This research was a part of an Aspasia programme and was supported by the Technology Foundation STW, applied science division of NWO and the technology programme of the Ministry of Economic Affairs.

REFERENCES

[1] American Iron and Steel Institute: *AISI Specification for the Design of Cold-Formed Steel Structural Members*, Washington, D.C., 1996.

[2] BAKKER, M.C.M.: *Web crippling of cold-formed steel members*, Proefschrift Technische Universiteit Eindhoven, 1992.

[3] BAKKER, M.C.M., ROSMANIT, M., HOFMEYER, H.: *Elastic Post-Buckling Behavior of Uniformly Compressed Plates*, 18th International Specialty Conference on Cold-Formed Steel Structures, Orlando, 2006.

[4] BAKKER, M.C.M., STARK, J.W.B: *Theoretical and Experimental Research on Web Crippling of Cold-Formed Flexural Steel Members*, Thin-Walled Structures, Vol. 18, Nr.4, 1994, pp. 261-290.

[5] CALLADINE, C.R.: *The Strength of Thin Plates in Compression*, In: Aspects of the Analysis of the Plate Structures: a volume in honour of Wittrick, W.H. Edited by Dawe, D.J., Horsinton, R.W., Little, A.G., Clarendon Press, Oxford, 1985.

[6] European Committee for Standardization: *ENV 1993-1-3, European Prestandard Eurocode3, Design of Steel Structures, Part 1-3: General rules-Supplementary rules for cold formed thin gauge members and sheeting*, CEN, Brussels, 1996.

[7] HOFMEYER, H.: *Web Crippling and Bending Moment Failure of First-Generation Trapezoidal Sheeting*, Experiments, Finite Element Models, Mechanical Models, Ph.D.- thesis, Eindhoven University of Technology, 2000.

[8] HOFMEYER, H., KERSTENS, J.G.M., SNIJDER, H.H. and BAKKER, M.C.M.: *New Prediction Model for Failure of Steel Sheeting Subject to Concentrated Load (Web Crippling) and Bending*, Thin Walled Structures, Vol. 39, Nr.9, 2001, pp. 773-796.

[9] HOFMEYER, H., ROSMANIT, M., BAKKER, M.C.M.: *Parameter study for first-generation sheeting failure using a theoretical and a FE model*, 18th International Specialty Conference on Cold-Formed Steel Structures, Orlando, Florida, 2006.

[10] LITTLE, G.A.: *The collapse of rectangular steel plates under uniaxial compression*, The Structural Engineer, Vol. 58B, No.3, 1980, pp. 45-61.

[11] MAHENDRAN, M.: *Local Plastic Mechanisms in Thin Steel Plates Under In-Plane Compression*, Thin Walled Structures, Vol. 27, Nr.3, 1997, pp. 245-261.

[12] MARGUERRE, K.: *Zur Theorie der gekrümmter Platte grosser Formänderung*, Proc. 5th Int. Congress for Applied Mechanics, Cambridge, UK, 1938.

[13] MURRAY, N.W.: *Introduction to the Theory of Thin-Walled Structures*, Oxford Engineering Science Series 13., Clarendon Press, Oxford, 1986.

[14] RHODES, J.: *Effective Widths in Plate Buckling, In: Developments in Thin-Walled Structures-1*, Edited by Rhodes, J. and Walker, A.C., Applied Science publishers, London, 1982.

[15] ROSMANIT, M., BAKKER, M.C.M.: *Report on Elastic Post-Buckling Behavior of Uniformly Compressed Plates*, Research Paper O-2006.02, Department of Architecture, Structural Design Group, Technische Universiteit Eindhoven, The Netherlands, 2006-a.

[16] ROSMANIT, M., BAKKER, M.C.M.: *Report on Post-Buckling Strength of Uniformly Compressed Plates*, Research Paper O-2006.03, Department of Architecture, Structural Design Group, Technische Universiteit Eindhoven, The Netherlands, 2006-b.

[17] WILLIAMS, D.G., WALKER, A.C.: *Explicit Solutions for the Design of Initially Deformed Plates Subjected to Compression*, Proc. Instn. Civ. Engrs. Part 2.59, 1975, pages 763-787.

Oponentní posudek vypracoval:

Doc. Ing. Tomáš Vraný, CSc., ČVUT Praha